Published online 29 December 2009 *Nucleic Acids Research, 2010, Vol. 38, No. 6* ***1853–1865***
doi:10.1093/nar/gkp1175

A novel function for the Mre11-Rad50-Xrs2 complex in base excision repair

Sylvia Steininger, Fred Ahne, Klaudia Winkler, Anja Kleinschmidt, Friederike Eckardt-Schupp and Simone Moertl*

Institute of Radiation Biology, Helmholtz Centre Munich – German Research Centre for Environmental Health, Ingolstaedter Landstrasse 1, D-85764 Neuherberg, Germany

Received September 18, 2009; Revised and Accepted December 1, 2009

ABSTRACT

The Mre11/Rad50/Xrs2 (MRX) complex in *Saccharomyces cerevisiae* has well-characterized functions in DNA double-strand break processing, checkpoint activation, telomere length maintenance and meiosis. In this study, we demonstrate an involvement of the complex in the base excision repair (BER) pathway. We studied the repair of methyl-methanesulfonate-induced heat-labile sites in chromosomal DNA *in vivo* and the *in vitro* BER capacity for the repair of uracil- and 8-oxoG-containing oligonucleotides in MRX-deficient cells. Both approaches show a clear BER deficiency for the *xrs2* mutant as compared to wildtype cells. The *in vitro* analyses revealed that both subpathways, long-patch and short-patch BER, are affected and that all components of the MRX complex are similarly important for the new function in BER. The investigation of the epistatic relationship of *XRS2* to other BER genes suggests a role of the MRX complex downstream of the AP-lyases Ntg1 and Ntg2. Analysis of individual steps in BER showed that base recognition and strand incision are not affected by the MRX complex. Reduced gap-filling activity and the missing effect of aphidicoline treatment, an inhibitor for polymerases, on the BER efficiency indicate an involvement of the MRX complex in providing efficient polymerase activity.

INTRODUCTION

In all organisms, the genome is continuously damaged by endogenous and exogenous factors, such as reactive oxygen species (ROS) or alkylating and oxidizing agents. Frequently, purine and pyrimidine moieties are damaged yielding base lesions that can lead to mutations (1,2). 8-oxoguanine (8-oxo-G) is the most frequent base damage induced by hydrogen peroxide (H_2O_2) (3,4), whereas alkylating agents such as methyl methanesulfonate (MMS) modify bases by adding methyl groups to nucleophilic sites. The predominant forms of MMS-induced DNA damage are the N-methylation adducts 7-methylguanine and 3-methyladenine (5). Spontaneous depurination of methylated purines leads to the formation of abasic (AP) sites, which are heat-labile, due to breakage of the phosphodiester bond at clustered damage. Presence of unrepaired AP sites result in cytotoxicity and mutagenicity, as well as blocks in DNA replication and transcription (6).

Repair of damaged bases and AP sites is normally carried out by the base excision repair (BER) system. In patients with defects in BER the failure to repair base damage can lead to malignancies and is associated with age-related degenerative diseases (7). BER is initiated by specific DNA *N*-glycosylases that recognize and excise the damaged bases to produce AP sites (8). In the major BER subpathway in *Saccharomyces cerevisiae* AP sites are then incised by the AP-endonucleases Apn1 and Apn2 creating a 5′-deoxyribophosphate (5′-dRP) end at the site of damage (9,10). The removal of the blocked 5′-end is catalyzed by Rad27. This protein is a specific 5′-flap endonuclease extending the AP sites to gaps of up to 5 nt (11,12). New DNA synthesis and subsequent ligation by Cdc9 complete BER (13). In an additional BER subpathway the damaged bases are processed by a DNA *N*-glycosylase/AP-lyase. In *S. cerevisiae* three enzymes with combined *N*-glycosylase-/AP-lyase activities are known that catalyze the excision of oxidized bases, namely Ogg1, Ntg1 and Ntg2 (14). 7-methylformamide pyrimidine, produced by MMS treatment, is excised efficiently by Ntg1 and Ntg2 (15). These enzymes produce 3′-α,β-unsaturated aldehydic (3′-dRP) ends, which pose a problem for DNA integrity because they cannot be extended by polymerases. Genetic studies suggest that the AP-endonucleases Apn1 and Apn2 contribute to the

*To whom correspondence should be addressed. Tel: +49 89 3187 3143; Fax: +49 89 3187 3378; Email: moertl@helmholtz-muenchen.de

removal of 3′-dRP by their 3′-phosphodiesterase activity (13). Afterwards, the gap is filled by polymerase activity and the original state is reconstituted by the ligase Cdc9 (13). In the case of the repair by AP-lyases, the repair patch length is not entirely clear (13). However, since elimination of the blocked 3′-end creates only a 1-nt gap, it is designated as the short-patch repair pathway (13,16). The nucleotide excision repair pathway components Rad1 and Rad10 provide a backup-pathway for 3′-dRP removal (13). Following the action of an AP-endonuclease, more than 1 nt is incorporated; therefore, this subpathway is called the long-patch BER (13). The polymerases that are involved in the BER process in yeast are not known. Wang *et al*. (17) could show that DNA synthesis during repair is carried out mainly by polymerase ε, but both, polymerase α and δ show modulating influences. In another report, polymerase δ was found to be the main enzyme for DNA synthesis after base damage by methylating agents (18).

In this article, we address the question of whether Xrs2 also has a direct role in the complex system of BER. Xrs2 is the yeast homolog to human Nbs1. Together with Mre11 and Rad50, it forms a trimeric complex (MRX) that is important for damage recognition and processing after DNA double-strand break (DSB) induction (19–22). Moreover, the complex plays a role in non-homologous end-joining (NHEJ) and homologous recombination (23,24). Besides its function in DSB repair, the MRX complex also affects many other cellular processes, including cell cycle checkpoint activation, telomere length maintenance and meiosis (25). Strains with mutations in *RAD52* group genes, including *XRS2*, are shown to be sensitive to MMS and H_2O_2 treatment (26–29). Furthermore, it was shown that *rad52* and *xrs2* deletion strains exhibit an increased mutation frequency compared to wildtype cells (15,30). Nevertheless, these genes were never mentioned to be directly linked to the BER pathway. It was assumed that unrepaired base damage or BER intermediates can lead to stalled replication forks which can be converted into DSBs. In addition, clustered DNA base damage and AP sites can induce DSB (28,31,32). Therefore, it was supposed that recombination-deficient cells are sensitive to base-damaging agents due to their role in homologous recombination as tolerance pathway for unrepaired base damage (13,33,34).

In this study, we demonstrated a direct role of the yeast MRX complex in the BER process, which contributes to resistance against base-damaging agents and to the avoidance of mutations. We showed that the repair capacity of MMS-induced heat-labile sites in stationary haploid cells is reduced in the *xrs2* mutant compared to wildtype, suggesting a BER defect. Consistently, decreased capacities in long-patch and short-patch BER were observed in cell extracts obtained from MRX deletion mutants using an *in vitro* assay. Subsequent analyses suggest the assignment of *XRS2* into the *NTG1*/*NTG2*-mediated BER subpathway as well as a function in facilitating polymerase activity required in BER. Thus, our results show for the first time a direct role for the MRX complex in BER.

MATERIALS AND METHODS

Yeast strains and media

The haploid *S. cerevisiae* strains used in this study are listed in Table 1. Strains are isogenic derivates of MKP-0, originally obtained from B.A. Kunz (Geelong, Australia). Deletion strains were constructed by gene replacement of the open reading frame and *in vivo* recombination (35) using polymerase chain reaction (PCR) products of the cassettes *KANMX6* and *HIS3MX6* (36) or the selectable markers *LEU2*, *TRP1* and *URA3*. All mutations were confirmed by PCR analysis. Construction and validation of mutants with truncated *XRS2* alleles are described previously (24). Strains used to measure mutation frequencies are derivates of BY4741 (37).

Standard medium yeast extract peptone dextrose (YEPD), containing 2% dextrose, 1% yeast extract and 2% peptone, was used as complete growth medium for yeast. Synthetic complete (SC) medium (2% dextrose; 0.6% yeast nitrogen base and the appropriate nutrients added) was used for yeast transformations performed by the lithium acetate method (38). SC medium lacking one nutrient allowed selection for the corresponding wildtype gene. For solid media, 2% agar was added. Canavanine plates were prepared by dissolving 60 mg canavanine (Sigma) in 1 l SC medium lacking arginine. For MMS plates, the agent was dissolved in concentrations ranging from 0.0025 to 0.02% in YEPD agar prior to pouring. All chemicals for media were purchased from Difco.

Analysis of mutation frequency

To measure mutation frequencies we used the strain BY4741 that carries a wildtype *CAN1* gene. Forward mutations in this gene lead to resistance to the arginine analog canavanine. For chemical-induced mutagenesis, overnight cultures were used to inoculate fresh YEPD medium with 2.5×10^6 cells/ml and incubated until they reached a cell titer of about 1×10^7 cells/ml. For MMS treatment, cells were incubated for 0, 10, 20 and 30 min with 0.1% MMS (Sigma) at 30°C. Afterwards, the cells were washed twice with and resuspended in potassium phosphate buffer (25 mM KPO_4, pH 7.0). For H_2O_2 treatment, the cells were resuspended in M9 buffer (39) containing 0, 1, 3 and 5 mM H_2O_2 (Merck). Following incubation at 30°C for 20 min, the reaction was stopped by adding 500 U/ml catalase (Sigma). To score for cell survival, the cells were plated onto YEPD and, to screen for Can^R (canavanine resistant) mutants, spread onto selective canavanine plates. The mutation frequencies are displayed as Can^R mutants per 10^7 surviving cells.

Exposure to DNA-damaging agents

The sensitivity of yeast strains to MMS and H_2O_2 was measured in the exponential growth phase. Overnight cultures were diluted in fresh YEPD medium to a density of 3×10^6 cells/ml and allowed to grow at 30°C with agitation to about 1×10^7 cells/ml. Cells were then treated with 0.2% MMS for 0, 15, 30 and 45 min at 30°C, pelleted and washed once with YEPD. For the survival

Table 1. *Saccharomyces cerevisiae* strains used in this study

Strain	Genotype	Reference
MKP-0	*MATα*, *can1-100*, *ade2-1*, *lys2-1*, *ura3-52*, *leu2-3-112*, *his3-Δ200*, *trp1-Δ901*, *RAD*	BA. Kunz
MKP-0 *Δxrs2*	Derivative of MKP-0 with *XRS2*::*KANMX6*	(24)
MKP-0 *xrs2-228M*	Derivative of MKP-0 *Δxrs2* with *xrs2-228M*	(24)
MKP-0 *xrs2-630*	Derivative of MKP-0 *Δxrs2* with *xrs2-630*	(24)
MKP-0 *Δapn1*	Derivative of MKP-0 with *APN1*::*Leu2*	This study
MKP-0 *Δapn1Δxrs2*	Derivative of MKP-0 with *APN1*::*Leu2*, *XRS2*::*KANMX6*	This study
MKP-0 *Δntg1Δntg2*	Derivative of MKP-0 with *NTG1*::*URA3*, *NTG2*::*TRP1*	This study
MKP-0 *Δntg1Δntg2Δxrs2*	Derivative of MKP-0 with *NTG1*::*URA3*, *NTG2*::*TRP1*, *XRS2*::*HIS3MX6*	This study
MKP-0 *Δapn1Δntg1Δntg2*	Derivative of MKP-0 with *APN1*::*Leu2*, *NTG1*::*URA3*, *NTG2*::*TRP1*	This study
MKP-0 *Δapn1Δntg1Δntg2Δxrs2*	Derivative of MKP-0 with *APN1*::*Leu2*, *NTG1*::*URA3*, *NTG2*::*TRP1*, *XRS2*::*HIS3MX*	This study
MKP-0 *Δmre11*	Derivative of MKP-0 with *MRE11*::*HIS3MX6*	(24)
MKP-0 *Δrad50*	Derivative of MKP-0 with *RAD50*::*LEU2*	(24)
BY4741	*MATa*; *his3Δ1*; *leu2Δ0*; *met15Δ0*; *ura3Δ0*	Euroscarf
BY4741 *Δxrs2*	*MATa*; *his3Δ1*; *leu2Δ0*; *met15Δ0*; *ura3Δ0 with xrs2::KANMX6*	Euroscarf

after H_2O_2 treatment, aliquots of 1 ml were incubated for 20 min with H_2O_2 concentrations ranging from 0 to 60 mM as described by Melo *et al*. (39). The addition of 500 U/ml catalase stopped the reaction. Appropriate dilutions were spread on YPED agar. After plating, cells were incubated for 3–5 days at 30°C. Survival was calculated by the ratio of the number of colonies after treatment versus the number of colonies without treatment.

For a crude analysis of the MMS sensitivity, cells in exponential growth phase were diluted serially in potassium phosphate buffer (25 mM KPO_4, pH 7.0), and aliquots of 5 µl were spotted on YEPD agar supplemented with 0.0025–0.02% MMS.

Repair of heat-labile sites after MMS treatment

The efficiency to repair heat-labile sites after MMS treatment *in vivo* was measured in haploid yeast cells under non-growth conditions. To obtain highly stationary yeast cells with a maximum of 3% budding cells, a modified cultivation protocol of Pohlit and Heyder (40) was used. Cells were collected, diluted in potassium phosphate buffer (25 mM KPO_4, pH 7.0) to a density of 7.5×10^8 cells/ml and treated for indicated time points with 0.1% MMS, followed by washing twice with potassium phosphate buffer. Afterwards, the samples were diluted in liquid holding recovery (LHR) buffer (100 mM glucose, 67 mM KPO_4, pH 5.0) (41–43) to a final density of 7.5×10^6 cells/ml and incubated at 30°C. The cells were embedded into agarose plugs before and after LHR incubation and genomic DNA was prepared according to Friedl *et al*. (43). During incubation at 55°C for proteinase K digestion MMS-induced clustered heat-labile sites are converted into DSB (31). Incubation at 32°C for the digestion step was used to check the basal level of chromosomal degradation. Chromosomal DNA was separated by pulsed-field gel electrophoresis (PFGE). The evaluation of residual damage was carried out with the software *Geltool*, that calculates profile values (pv's) representing the extent of chromosomal degradation. Details were described previously (24).

Preparation of cell-free protein extracts

Fifty milliliters of YEPD was inoculated with a single colony and the culture was grown to stationary growth phase at 30°C. The pre-culture was diluted 10-fold with YEPD medium and incubated under vigorous shaking at 30°C to early logarithmic growth phase ($5 \times 10^6 - 1 \times 10^7$ cells/ml). The cells were kept on ice for 20 min, centrifuged (4000 r.p.m., 4°C, 20 min) and washed twice with potassium phosphate buffer (25 mM KPO_4, pH 8.0). Afterwards, the cell pellet was resuspended in 5 ml ice-cold extraction buffer (100 mM Tris–HCl, pH 8.0; 10 mM β-mercaptoethanol) and 1 ml protease inhibition mix (Sigma) was added per 20 g of cell pellet. Cells were crushed by using a pre-chilled French Press Cell (Aminco) applying an internal pressure of 20 000 psi. The crude extract was adjusted to pH 8.0 by adding 0.1 M NaOH and the cell debris was removed by centrifugation at 20 000 r.p.m. in a SS34 rotor for 40 min at 4°C. The supernatant was carefully removed without disturbing the pellet. Protein was precipitated by stepwise addition of ammonium sulfate to a concentration of 0.35 g/ml for at least 20 min on ice, collected by centrifugation (20 000 r.p.m., 30 min, 4°C), dissolved in 3 ml dialysis buffer (10 mM Tris–HCl, pH 7.5; 10 mM β-mercaptoethanol) and then dialyzed overnight at 4°C against the same buffer. The extract was further centrifuged for 10 min to remove insoluble particles. The crude extract was either used directly or stored for up to 6 months at –80°C before use. Protein concentrations were determined according to Bradford using BSA as standard.

Preparation of substrates for *in vitro* assays

For *in vitro* BER assays, single-strand (ss)DNA oligonucleotides (35-mer) containing a uracil residue (BER1 = 5′-GCC CTG CAG GTC GAU TCT AGA GGA TCC CCG GGT AC-3′) or an 8-oxoG (BER3 = 5′-GCC CTG CAG GTC GAG$^{8\text{-oxo}}$ TCT AGA GGA TCC CCG GGT AC-3′) at position 15 were annealed to their complementary synthetic strands (BER2 = 5′-GTA CCC GGG GAT CCT CTA GAG TCG ACC TGC AGG GC-3′ and BER4 = 5′-GTA CCC GGG GAT CCT CTA GAC

TCG ACC TGC AGG GC-3′). Annealing was performed by mixing equimolar amounts of both oligonucleotides and incubating them for 10 min at 95°C followed by slow cooling down to room temperature. For the *in vitro* incision assay BER1 was labeled prior to annealing using T4 polynucleotide kinase (MBI-Fermentas) and [γ-^{32}P]ATP according to the manufacturer's instructions. Afterwards, the substrate was purified using G-25 Sephadex minicolumns (Roche) to remove unincorporated [γ-^{32}P]ATP. To measure the gap-filling activity of cell extracts, a 14-nt ssDNA oligonucleotide (BER5 = 5′-GCC CTG CAG GTC GA-3′) was labeled, while the 5′-end of a 17–nt-long oligonucleotide (BER6 = 5′-AGA GGA TCC CCG GGT AC-3′) was non-radioactively phosphorylated. The annealing of BER5 and BER6 to BER2 generated a repair substrate lacking 4 nt in one strand.

In vitro repair assays

To determine the BER capacity of cell-free extracts, an *in vitro* BER assay was performed according to Harrigan *et al*. (44). Briefly, 20 µg protein were dissolved in BER reaction buffer (50 mM HEPES, pH 7.5; 0.5 mM EDTA; 2 mM dithiothreitol; 20 mM KCl; 4 mM ATP; 5 mM phosphocreatine; 0.5 mM NAD^+; 0.1 mM ddTTP; 100 µg/ml freshly prepared phosphocreatine kinase) and preincubated with 250 nM oligonucleotide substrate (BER1 + BER2 or BER3 + BER4) for 5 min at room temperature. Addition of 2.2 µM [α-^{32}P]dCTP and 10 mM $MgCl_2$ initiated the repair reaction and the samples were incubated at 37°C for the indicated time points. The reactions were stopped by adding 5 mM EDTA and heating for 5 min to 72°C. Purification with G-25 Sephadex minicolumns (Roche) according to the manufacturer's instructions was done to remove unincorporated [α-^{32}P]dCTP. Afterwards, repair substrates were mixed with an equal volume of DNA loading dye (95% formamide; 20 mM EDTA; 0.02% bromphenol blue; 0.02% xylene cyanol) and incubated for 2 min at 72°C. For inhibition of polymerases protein extracts were preincubated for 30 min at 30°C with 2 µg/ml aphidicoline.

The *in vitro* incision assay was carried out on the basis of Wang *et al*. (45). Two-hundred and fifty nanomoles of oligonucleotide substrate ([γ-^{32}P]BER1 + BER2) were incubated in 10 µl incision reaction buffer (50 mM HEPES, pH 7.7; 7.5 mM $MgCl_2$; 0.5 mM EDTA; 1 mM dithiothreitol; 20 mM phosphocreatine; 2% glycerol; 100 µg/ml bovine serum albumin) with 1 µg cell free protein extract for the indicated time points at 23°C. The reactions were terminated by adding 20 µl stop solution (250 mM HEPES, pH 7.5; 1% sodium dodecyl sulfate (SDS); 500 µg/ml proteinase K) and heating for 20 min to 60°C. Repair products were ethanol-precipitated and solubilized in DNA loading dye as mentioned above.

For the gap-filling assay, 40 µg cell extract were mixed with 10 nM oligonucleotide substrate (BER2 + [γ-^{32}P]BER5 + BER6) and reaction buffer (50 mM Tris, pH 7.4; 50 mM KCl; 1 mM dithiothreitol; 5 mM $MgCl_2$; 5% glycerol). 2.5 mM dCTP and 2.5 mM dTTP were added. Reactions were stopped by adding 5 mM EDTA, mixed with 10 µl loading dye and heated for 5 min to 72°C.

All repair products were separated by polyacrylamide gel electrophoresis (24% acrylamide for the BER assay and the gap-filling assay and 18% acrylamide for the incision assay; 8 M urea; 89 mM Tris–HCl, pH 8.8; 89 mM boric acid; 2 mM EDTA), detected by autoradiography and quantified by digital imaging (TotalLab, Amersham).

RESULTS

Deletion of *XRS2* leads to high mutation frequency and MMS sensitivity

Mutations in *RAD52* group genes lead to increased sensitivities to alkylating and oxidizing agents (26–28) and a genome-wide screen showed increased mutation frequencies after MMS treatment (15,30). We verified these findings in our experimental systems for the deletion of *XRS2* and *RAD52*. Both, the *xrs2* mutant and the recombination-deficient mutant *rad52,* conferred a high sensitivity to MMS and H_2O_2, whereas the *xrs2* mutant shows an even higher sensitivity to H_2O_2 treatment as compared to the *rad52* mutant (Figure 1A and B). Mutation frequencies were determined with a forward mutation system leading to canavanine resistance (Figure 1C and D). In wildtype cells, the spontaneous mutation frequency averaged 20 Can^R mutants per 10^7 cells, while deletion of *XRS2* increased the frequency 5–6-fold to 100–120 mutants per 10^7 cells. Furthermore, *xrs2* mutants exhibited an elevated mutation frequency after MMS treatment. Following incubation for 30 min in 0.1% MMS the number of Can^R mutants in the *xrs2* strain was raised to 550 per 10^7 survivors, while in wildtype cells the number increased only to 200 Can^R mutants. Mutation frequencies were also increased in the *xrs2* mutant after H_2O_2 treatment. Incubation in 5 mM H_2O_2 yielded 130 mutants per 10^7 survivors in wildtype cells and 260 mutants per 10^7 survivors in the *xrs2* deletion mutant. These results emphasized the importance of *XRS2* and *RAD52* to preserve genomic stability after treatment with base damaging agents.

Xrs2 plays a role in the repair of heat-labile sites after MMS treatment

For many years, MMS was used as radiomimetic agent, to introduce DSB into DNA (46). New results, however, showed that MMS-induced DSB, which can be detected by PFGE, are due to elevated temperatures in DNA preparation where MMS-induced heat-labile sites are converted to DSB (31,47). We used this method to investigate the repair of MMS-induced heat-labile sites in stationary cells from wildtype, *xrs2* and *rad52* deletion strains. We determined the residual DNA damage 23 h after MMS treatment with 0.1% MMS for 0, 10, 20, 40 and 60 min. DNA damage repair was facilitated by incubating the cells under non-growth conditions (LHR), which allows DNA repair while proliferation is suppressed (41–43). Residual heat-labile sites were converted into DSB during proteinase K incubation at 55°C for DNA

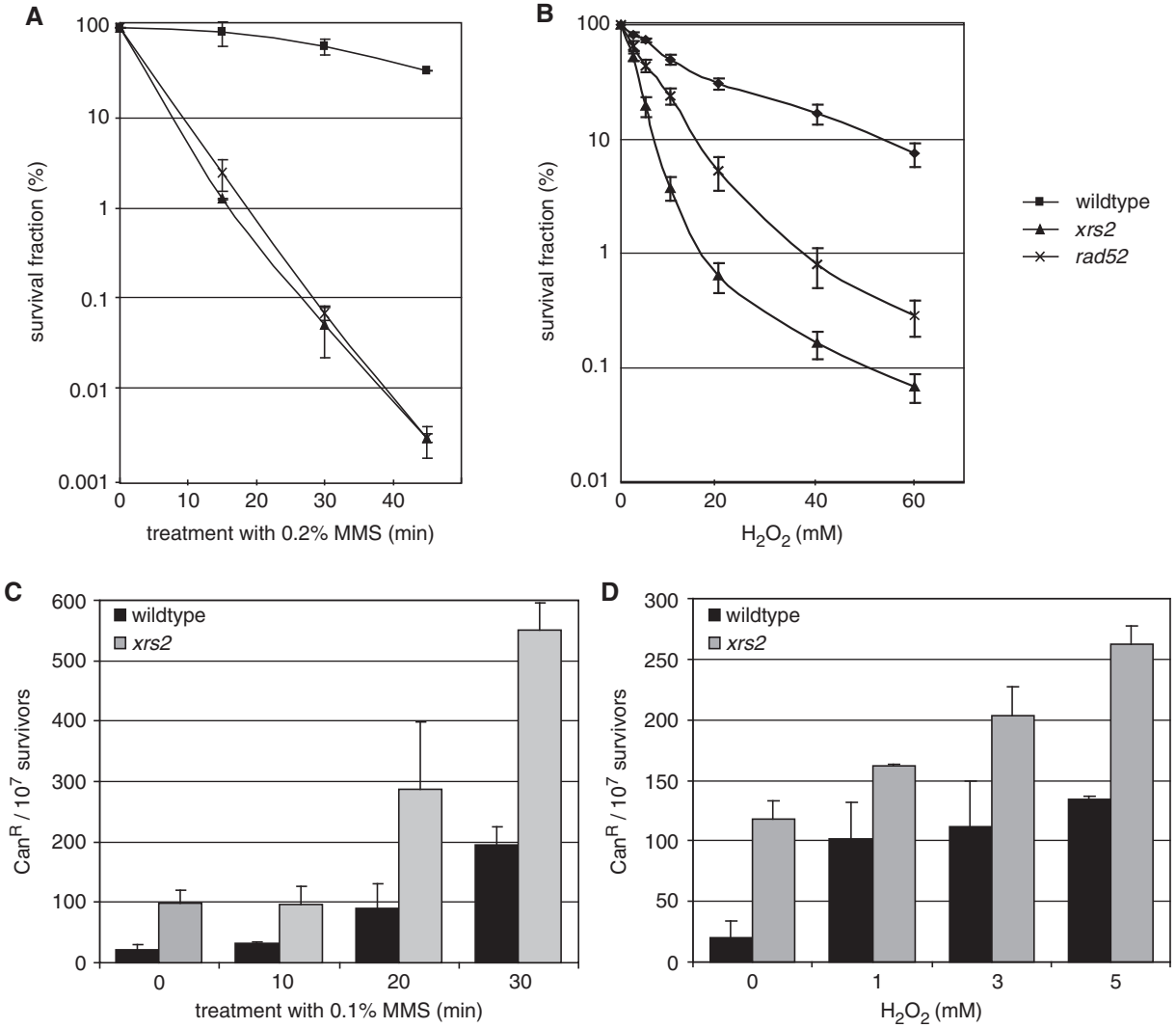

Figure 1. Sensitivity to base-damaging agents and mutation frequencies. (**A, B**) Sensitivity of the *xrs2* deletion mutant to MMS and H_2O_2 compared to MKP-0 wildtype and the *rad52* deletion mutant. Survival was plotted as the ratio of colonies obtained after treatment versus colonies obtained without treatment. (**C, D**) Induced mutation frequencies of BY4741 wildtype and its isogenic *xrs2* deletion mutant after MMS and H_2O_2 treatment shown as canavanine-resistant (Can^R) mutants per 10^7 survivors. Results are an average of three independent experiments ± SD.

agarose plug preparation. As a control, DNA plugs were also prepared at 32°C. The resulting gel showed distinct bands of chromosomal DNA and little background in untreated and MMS-treated samples prepared at 32°C from both, wildtype and *xrs2* strains (Figure 2A). This result indicated that there were equally low levels of DSB in wildtype and in the *xrs2* mutant, and no direct induction of DSB by MMS was detectable in both strains. The results for DNA preparation at 55°C 0 h and 23 h after irradiation are shown in Figure 2B. Immediately after MMS treatment, the DNA fragmentation increased dependent on the length of MMS treatment. Twenty-three hours after incubation under LHR conditions, DNA repair was visible as the reappearance of chromosomal bands. To quantify the extent of chromosomal degradation we used the software program *Geltool* (24) and the residual damage was plotted against the time of MMS treatment (Figure 2C). Dependent on treatment time, the amount of residual damage increased moderately in wildtype (slope of regression line 0.0268), while there was a more pronounced accumulation of residual damage in the *xrs2* mutant (slope of regression line 0.0527). In line with a recent publication (31), we found that the HR-deficient *rad52* mutant shows a repair activity comparable to wildtype cells (slope of regression line 0.0304). Relative quantification of slopes of regression lines showed a 2-fold enhanced increase in the *xrs2* mutant (Figure 2D). Furthermore, the *xrs2* mutant exhibited a marginally increased amount of heat-labile sites in untreated cells. Therefore, the reduced ability of the *xrs2* mutant to repair MMS-induced heat-labile sites was not due to reduced recombinational repair, a backup pathway for the repair of DNA base damage.

Xrs2 is directly involved in the BER pathway

The results from the analysis of MMS-induced heat-labile sites suggested an involvement of *XRS2* in the repair of DNA base damage. To further elucidate this assumption

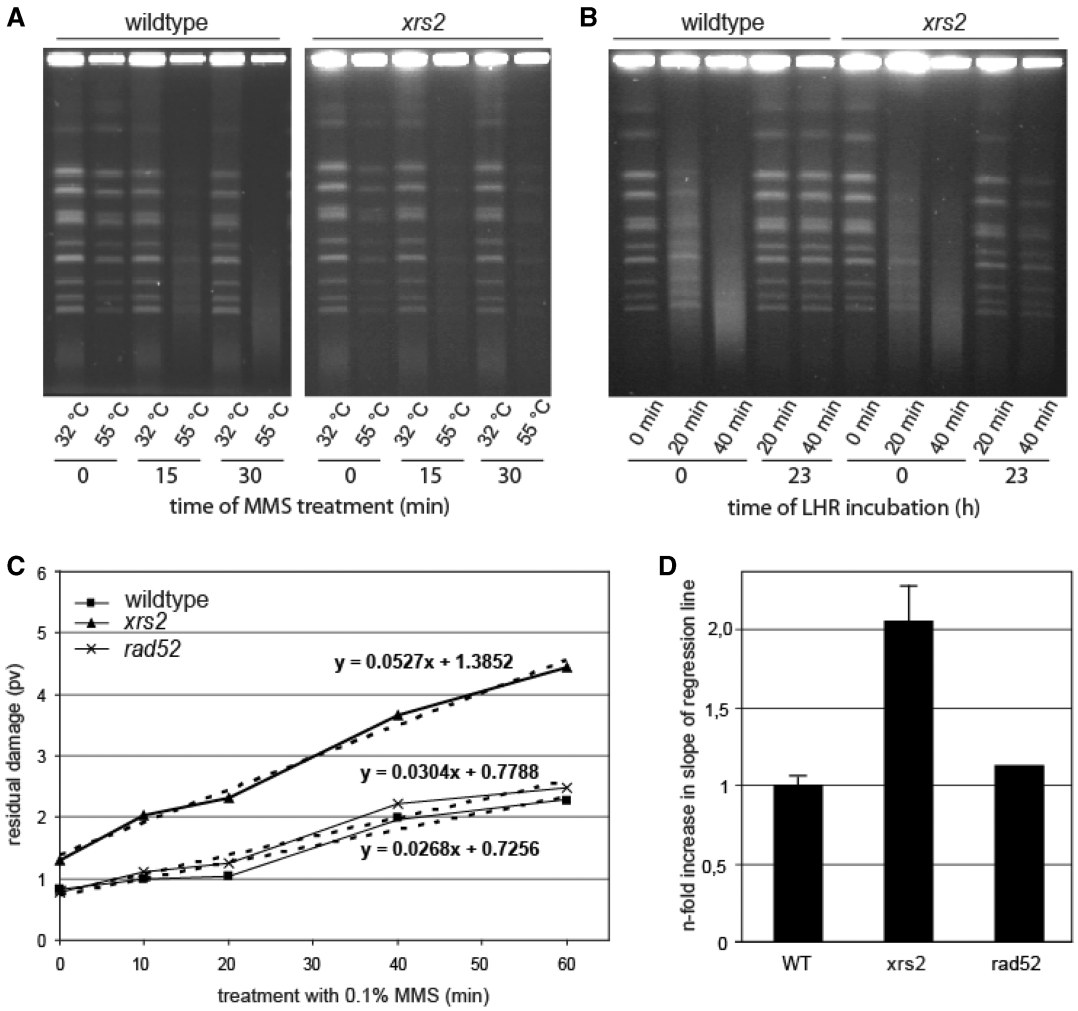

Figure 2. Analysis of the repair of heat-labile sites. (**A**) Induction of chromosomal degradation in wildtype and the *xrs2* mutant visualized by pulsed-field gel electrophoresis. Cells were treated for 0, 15 and 30 min with 0.1% MMS. During preparation of chromosomal DNA, the incubation with proteinase K was carried out at 32°C (heat-labile sites remain stable) as well as 55°C (heat-labile sites are converted into DSB). (**B**) Analysis of chromosomal degradation (proteinase K incubation at 55°C) immediately after treatment for 0, 20 and 40 min with 0.1% MMS as well as after 23 h incubation of the cells under LHR conditions. (**C**) Residual DNA fragmentation plotted against the time of MMS treatment. The degree of residual chromosomal degradation was quantified using the software program *Geltool* and is shown as profile value (pv). Linear equations are calculated from regression lines (dashed lines). One representative experiment is shown. (**D**) Slope of regression lines obtained from residual chromosomal degradations from the *xrs2* and *rad52* mutant relative to wildtype. Mean values from three independent experiments for the *xrs2* mutant and for wildtype are shown. The *rad52* mutant was analyzed once.

we employed an *in vitro* BER assay according to Harrigan *et al.* (44) (Figure 3A). We analyzed the repair of 35-bp double-stranded oligonucleotides containing a uracil or an 8-oxoG at position 15. These substrates were incubated with the same amounts of protein extracted from wildtype cells and *xrs2* mutant cells in logarithmic growth phase. During the repair process damaged bases (uracil and 8-oxoG) are removed from the substrate and a [α-^{32}P]dCTP or a [α-^{32}P]dGTP was incorporated opposite G or C, respectively. Before ligation, this intermediate has a size of 15 nt; after ligation the original size of 35 nt was restored. To distinguish between short-patch repair, where only 1 nt is substituted, and long-patch repair, where a number of nucleotides were replaced, ddTTP is added to the reaction mixture to abort elongation. This allowed detecting long-patch repair products with a size of 16 nt. Using an error-free oligonucleotide, we observed no repair products (data not shown). Figure 3B shows a representative experiment for the repair of a uracil-containing oligonucleotide by cell extracts from wildtype cells and from the *xrs2* mutant. It has to be noted that exposure times were different for monitoring long-patch and short-patch repair. In line with current publications usage of equal exposure times revealed clearly higher amounts of long-patch products (13,48), but quantification was hardly possible (data not shown). The amount of all three detectable repair products (intermediate, long patch and short patch) were reduced in extracts obtained from the *xrs2* mutant. The formation of repair products was similarly reduced for an 8-oxoG containing oligonucleotide in the BER assay (Figure 3C). The quantitative examination of at least three independent

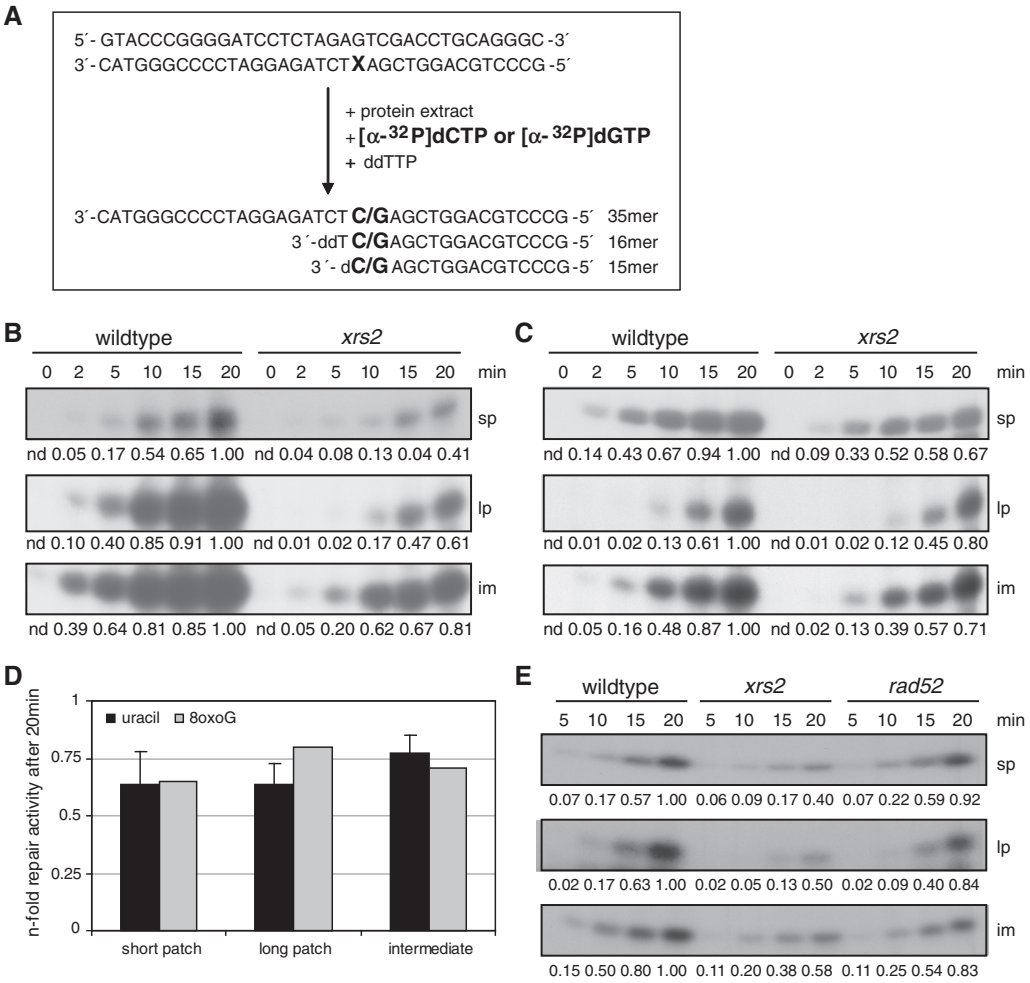

Figure 3. *In vitro* analysis of short-patch and long-patch BER with whole-cell extracts from wildtype cells and from the *xrs2* mutant. (**A**) Principle of the *in vitro* assay (X = uracil or 8-oxoG). Labeled repair products are generated by BER activity of whole cell extracts. (**B, C**) Repair capacities for the repair of the uracil-containing oligonucleotide (**B**) and the 8-oxoG-containing oligonucleotide (C) of cell extracts obtained from wildtype cells and from the *xrs2* mutant. The number below the images indicates the relative intensity of the corresponding band relative to the strongest band in that line. (**D**) Relative BER activity of the *xrs2* mutant after a 20-min repair time. The diagram shows the average of three independent experiments using the uracil-containing oligonucleotide; the results for the 8-oxoG-containing substrate were obtained from one experiment. (**E**) Analysis of the BER capacity in cell extracts from the *rad52* mutant in comparison to cell extracts from wildtype cells and the *xrs2* mutant using the uracil-containing substrate. One representative experiment out of three is shown. nd., not determined.

extracts showed that the amount of short-patch and long-patch products synthesized by *xrs2* extracts within 20 min was reduced to 0.64-fold the amount produced by wildtype extracts. The intermediate constituted 0.77-fold of the amount synthesized by wildtype extracts (Figure 3D). In contrast, extracts from the *rad52* mutant remained BER proficient (Figure 3E). For the first time, we demonstrated reduced BER capacity in cell free extracts from the *xrs2* mutant for the repair of both, uracil- and 8-oxoG-containing oligonucleotides.

The new role of Xrs2 in BER is a function of the whole MRX complex

Xrs2 forms a trimeric complex with Mre11 and Rad50 (49). To analyze whether the newly detected role of Xrs2 in BER is a function of Xrs2 alone, or of the whole MRX complex, we analyzed MMS sensitivity and *in vitro* BER capacity in *mre11* and *rad50* deletion mutants. Since it was previously shown that several N- and C-terminal truncated versions of *XRS2* exhibit MMS sensitivity (50), we also analyzed two recently constructed *xrs2* mutants (24) either lacking the FHA- and BRCT-domains at the N-terminus (*xrs2-228M*) or the Tel1- and Mre11-binding domains at the C-terminus (*xrs2-630*) for their BER capacity. Figure 4 shows that all mutants except the *xrs2-228M* mutant behaved like the *xrs2* mutant. Reduced BER capacities and increased sensitivity against MMS were equally evident for the *mre11*, *rad50* and *xrs2-630* mutant, and comparable to that seen in the *xrs2* deletion mutant. Thus, we concluded that the complete MRX complex is involved in the BER pathway and especially the Mre11-binding domain of Xrs2 is important, while the FHA- and the BRCT-domains have no function in BER.

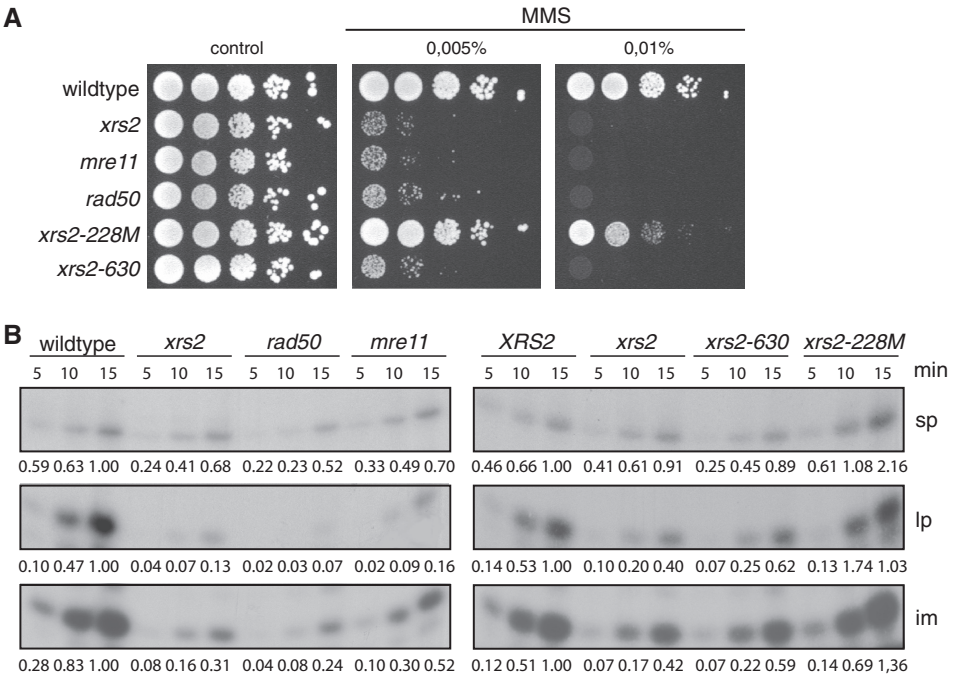

Figure 4. MMS sensitivity and BER capacity of MRX-deficient cells and mutants carrying truncated versions of the Xrs2 protein. (**A**) Analysis of the MMS sensitivity. Shown are serial dilutions of cells on plates containing MMS as indicated. (**B**) Repair capacity of cell extracts obtained from the *mre11*, the *rad50* mutant and from strains expressing truncated versions of *XRS2* compared to wildtype and the *xrs2* deletion mutant. The numbers below the images indicate the relative intensity of the corresponding band relative to the strongest band in that line. One of three independent experiments is shown.

Epistatic relationship of *XRS2* to other genes involved in BER

To assign the MRX complex to the AP-endonuclease or the AP-lyase subpathway we analyzed the epistatic relationship of *XRS2* and other BER genes concerning survival and *in vitro* BER capacity. We deleted *XRS2* in an *apn1* mutant, where the major BER pathway in yeast via the AP-endonuclease Apn1 is blocked. The AP-lyase pathway remains unaffected because in this mutant Apn2 can act as an efficient 3′-phosphodiesterase and compensate for the *APN1* deletion in this function (13). Furthermore, we deleted *XRS2* in the AP-lyase deficient mutant *ntg1ntg2*. Finally, we compared the quadruple mutant *xrs2apn1ntg1ntg2* to the triple mutant *apn1ntg1ntg2*. The *apn1* mutant exhibited a moderate MMS sensitivity (Figure 5A and B), while survival was hardly influenced by the deletion of *NTG1* and *NTG2* (Figure 5B). An effect of the *ntg1ntg2* deletion appeared after additional deletion of *apn1*, when both the AP-endonuclease and the AP-lyase subpathways were impaired. Additional deletion of *XRS2* in the *apn1* background enhanced the sensitivity. In contrast, deletion of *NTG1* and *NTG2* suppressed the high MMS sensitivity of the *xrs2* single mutant, resulting in the phenotype of the *ntg1ntg2* double mutant. Similarly, the *xrs2* phenotype was suppressed in the quadruple mutant *xrs2apn1ntg1ntg2* (Figure 5B).

Similar effects were observed in the *in vitro* BER assays (Figure 5C and D). The *apn1* mutant produced less intermediate and long-patch products when compared to wildtype, while the short-patch capacity was not influenced. The *apn1xrs2* double mutant showed an additive effect on long-patch BER activity, while the short-patch BER activity of the *xrs2* phenotype was observed. Compared to wildtype cells the *ntg1ntg2* mutant showed no BER defect. Moreover, the additional deletion of *XRS2* hardly influenced the repair capacity. For all three repair products the *xrs2* phenotype was almost completely suppressed. We also tried to analyze the *apn1ntg1ntg2* triple mutant and the *apn1ntg1ntg2xrs2* quadruple mutant for their BER capacity, but insufficient repair products were generated (data not shown). Therefore, it was not possible to draw a conclusion for the influence of an additional *XRS2* deletion. However, due to the additive effect of *APN1* and *XRS2,* as well as the suppressive effect, of the *NTG1* and *NTG2* deletion on the *xrs2* phenotype, we propose an involvement of the MRX complex downstream of the AP-lyases.

Functional analysis of the BER mechanism after deletion of *XRS2*

To analyze the efficiencies of base recognition and DNA incision at the AP site we carried out an *in vitro* base incision assay using the same uracil-containing substrate as in the BER assay labeled at the 5′-end. If the uracil is recognized and removed and the DNA is incised, a 14-nt and a 15-nt-long product is generated (Figure 6A). The specificity of the reaction was tested with different control approaches. Without cell extract no incision could be detected. The addition of exogenous recombinant uracil glycosylase (UDG) from *Escherichia coli* caused the removal of uracil, while the phosphate backbone was

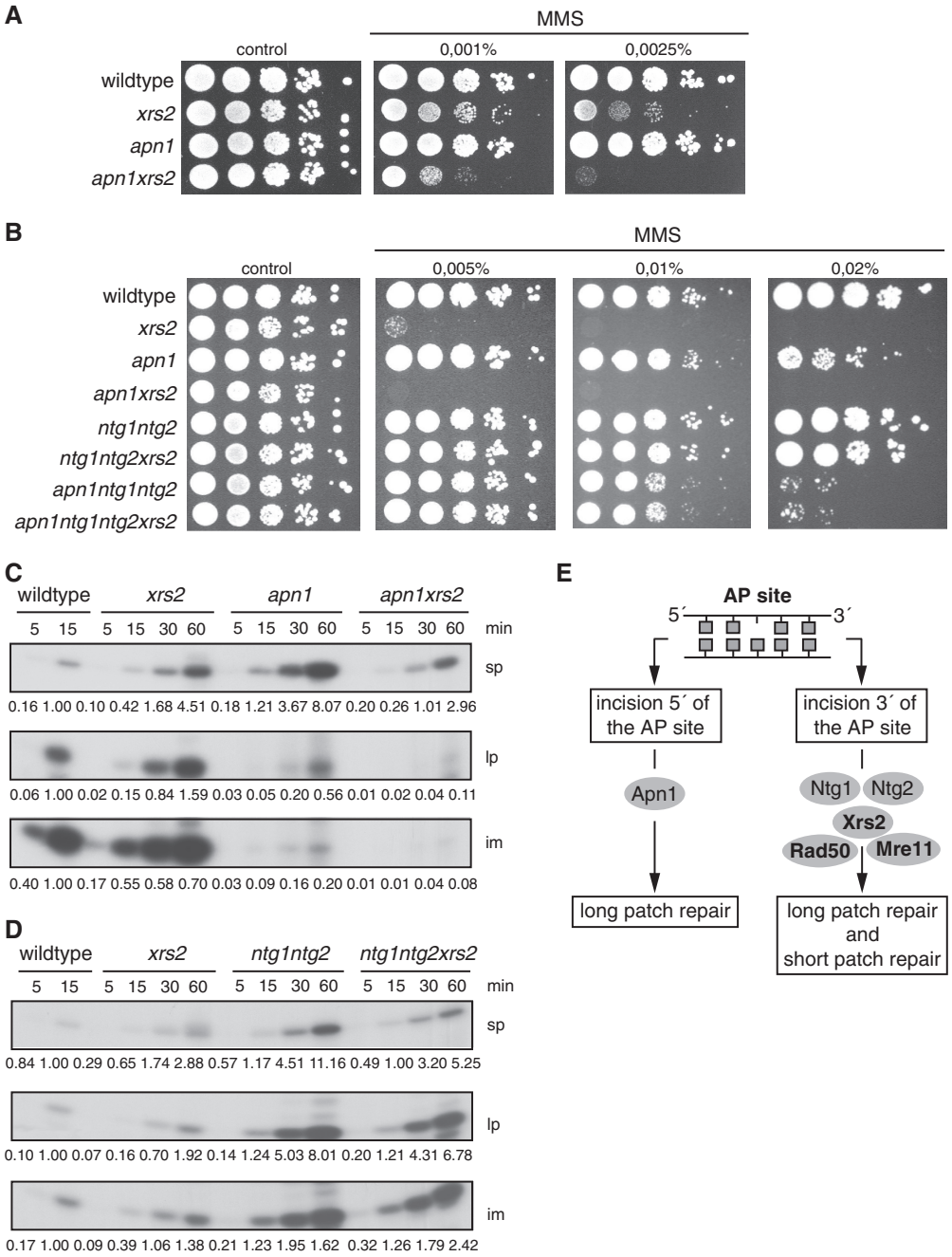

Figure 5. Epistatic relationship of *XRS2* to other BER genes. (**A**, **B**) Analysis of MMS sensitivity. Shown are serial dilutions of cells on plates containing MMS as indicated. (**C**) Repair capacity for the repair of the uracil-containing oligonucleotide of cell extracts obtained from the *apn1* and the *apn1xrs2* mutant compared to cell extracts from wildtype cells and from the *xrs2* single mutant. (**D**) Repair capacity for the repair of the uracil-containing oligonucleotide of cell extracts derived from the *ntg1ntg2* double mutants and *ntg1ntg2xrs2* triple mutant compared to cell extracts derived from wildtype cells and from the *xrs2* single mutant. In each case, one representative experiment out of three is shown. (**E**) Proposed model for the allocation of *XRS2* to the AP-lyase-mediated repair pathway. The phenotypes of the *apn1* and *xrs2* single mutants are combined in the *apn1xrs2* double mutant; otherwise, the effect of *xrs2* is suppressed in the *ntg1ntg2* mutant. These findings assign the MRX complex downstream of the AP-lyases where short-patch and long-patch repair products can be synthesized.

hydrolyzed by NaOH (Figure 6B, right part of image). Figure 6B (left part of image) shows that an extract from the *xrs2* mutant produced the same amount of incision product compared to an extract from wildtype cells. However, deletion of *APN1* led, as expected, to a clear defect in the incision assay (Figure 6B, middle part of image). Therefore, the first steps in BER, base recognition and DNA incision, were not influenced by Xrs2.

Following removal of the damaged base, the gap has to be filled by polymerase activity. To measure strand elongation reactions we carried out a gap-filling assay where the substrate mimics an intermediate of the long-patch

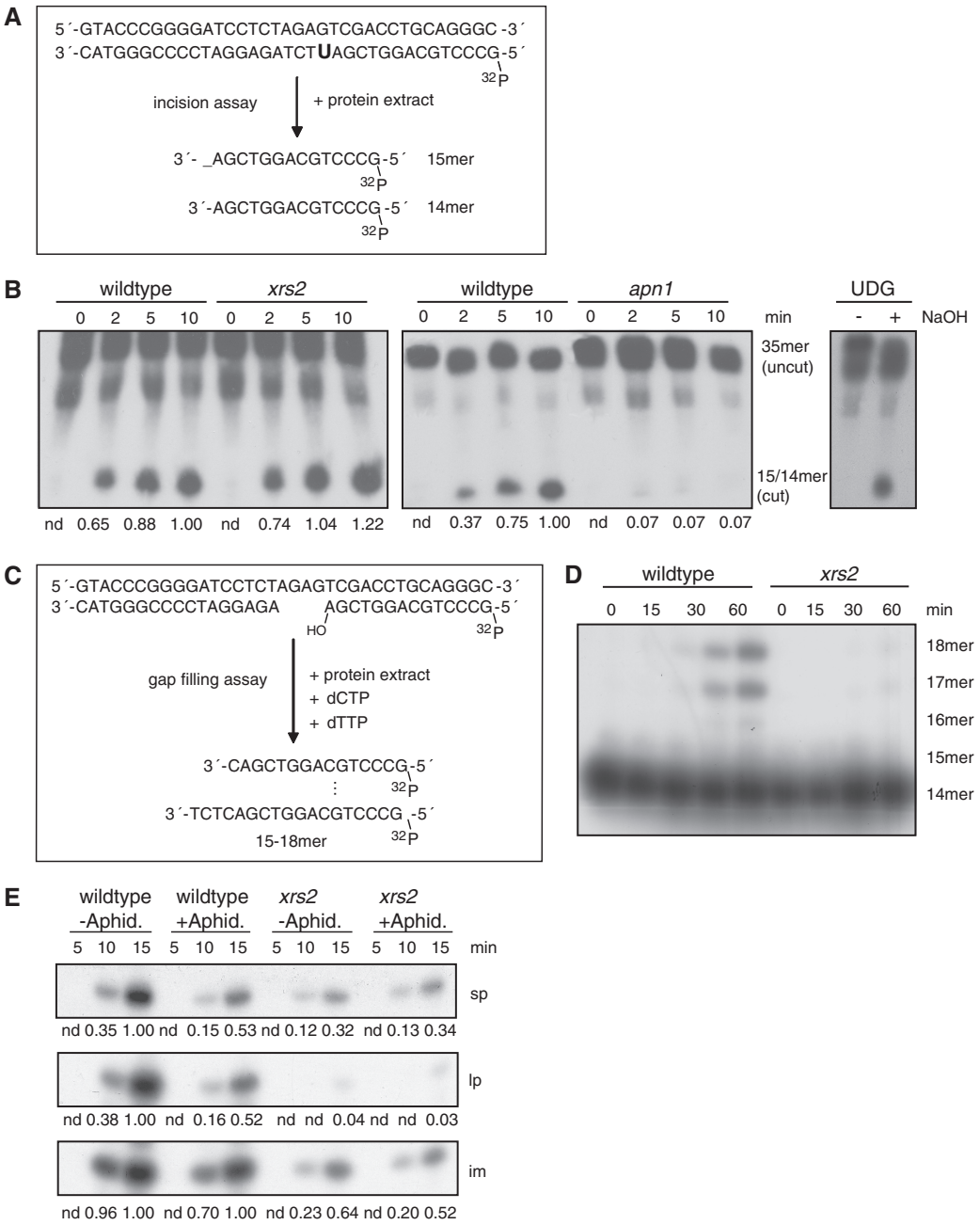

Figure 6. Analysis of individual steps in the BER process after deletion of *XRS2*. (**A**) Incision assay using the uracil-containing oligonucleotide. Generation of an AP site and incision activity can be monitored through the appearance of cut products of the labeled substrate. (**B**) Incision assay with whole-cell extracts derived from wildtype cells and form the *xrs2* (left part of image) and the *apn1* (middle part of image) mutant. Stability of the phosphodiester bond was demonstrated by using an UDG-treated (Uracil-DNA-Glycosylase) substrate. The successful generation of AP-sites after UDG-treatment was shown by hydrolyzing the phosphodiester bond under alkaline conditions (right part of image). (**C**) Four-nucleotide gap-filling assay; gap-filling activity is visible through the extension of the 5′-labeled substrate. (**D**) Gap-filling activity of cell extracts derived from the *xrs2* mutant compared to cell extracts from wildtype cells. (**E**) *In vitro* BER assay of whole-cell extracts from wildtype cells and from the *xrs2* mutant preincubated with 2 μg/ml aphidicoline for 30 min. In each case, one representative experiment out of three is shown.

pathway with a gap of 4 nt in one strand. Since no ATP for ligase activity was added the products can only reach a length of 15–18 nt (Figure 6C). Compared to wildtype the *xrs2* mutant showed decreased gap-filling activity (Figure 6D). While extracts from wildtype cells were able to fill in the missing 4 nt within 15 min, the *xrs2* mutant showed no strand elongation within 60 min incubation time. A further indication for reduced polymerase activity in the *xrs2* mutant can be seen in the *in vitro* BER assay with cell extracts supplemented with 2 μg/ml aphidicoline for the inhibition of polymerases (Figure 6E). In the wildtype extract, aphidicoline treatment reduced the amount of both, short-patch and long-patch product, 0.5-fold compared to mock-treated

samples. In samples with *xrs2* extract, however, aphidicoline treatment had no impact on strand elongation and polymerization activity was equally low in treated and untreated *xrs2* extracts. This indicates that the main part of new DNA synthesis in wildtype cells is executed by an aphidicoline sensitive polymerase, while the residual amount of repair synthesis in the *xrs2* mutant is done by an aphidicoline insensitive polymerase.

DISCUSSION

In this study, we demonstrated that fully active BER is dependent on an intact MRX complex activity in *S. cerevisiae*. This was evidenced by an impaired repair of chromosomal heat-labile sites, which are clusters of base damage, in the *xrs2* deletion strain. Furthermore, whole-cell extracts from strains containing deletions in MRX component genes displayed reduced repair efficiency in an *in vitro* BER assay as well as decreased gap-filling activity.

Deletion of *XRS2* led to an elevated spontaneous mutation frequency as well as to increased induced mutation frequency and increased sensitivities after MMS and H_2O_2 treatment (15,30). So far, this was explained by the role of the *RAD52* epistasis group genes facilitating recombinational repair as part of a tolerance pathway for stalled replication forks after base damage (28,31,32). However, we detected differences in the repair of MMS-induced chromosomal DNA damage between the *rad52* deletion mutant and the *xrs2* mutant. The *rad52* mutant repaired the induced damage within 23 h as efficiently as wildtype cells, consistent with the assumption that replication bypass and recombinational repair were less important in G1 haploid cells. In contrast, in the *xrs2* deletion mutant the residual damage was increased about 2-fold as compared to wildtype and the *rad52* mutant. As the assay detected damaged bases, abasic sites and intermediate breaks arising during BER (31,47), this observation hinted at a role for *XRS2* in BER that is independent of *RAD52*.

This assumption was further supported by the results of an *in vitro* BER assay modified from Harrigan *et al.* (44). Whole-cell extracts from the *xrs2* mutant showed only 60% of the repair capacity of wildtype or the *rad52* mutant within 20 min. Since it was possible to distinguish between short-patch and long-patch BER with this assay, we could show that both subpathways were equally affected by deletion of *XRS2*. Therefore, the function of *XRS2* in BER should be upstream of the branching of the two pathways. Alternatively, *XRS2* could be independently required for both subpathways. This BER defect can be seen in the repair of both, 8-oxoG and uracil, indicating a function for *XRS2,* independent of the native of the damaged base. Further analysis of *mre11* and *rad50* mutants demonstrated that the new function of Xrs2 is a function of the complete MRX complex. The *in vitro* BER capacity in all three mutants was decreased to a similar extend. In addition, we analyzed BER activity in mutants lacking the Mre11-binding domain or the N-terminus, including the FHA and BRCT domain of Xrs2, which were shown to be important for NHEJ (51). These experiments revealed that the truncation of the Mre11-binding domain was sufficient for the inactivation of the Xrs2 protein in BER.

To further elucidate the involvement of Xrs2 in BER, we investigated the epistatic relationship of *XRS2* to both BER subpathways. We combined the deletion of *XRS2* with deletions blocking either the AP-endonuclease-dependent long-patch repair pathway, which is most important in *S. cerevisiae* or the mechanistically less defined AP-lyase-mediated subpathway (13). In agreement with the current model of BER, the *APN1* deletion displayed a clear defect in long-patch BER. The *apn1xrs2* double mutant showed an additive effect in the long-patch repair and the *xrs2* defect in the short-patch repair. An additive effect was also observed for MMS sensitivity. Therefore, we concluded that *XRS2* and *APN1* act on different pathways concerning DNA base damage removal. Deletion of *NTG1* and *NTG2* had no effect on BER and survival after MMS. This was consistent with the minor importance of the AP-lyase-mediated BER pathway (7,13). Otherwise, the function of Ntg1 and Ntg2 could be replaced by other lyases, like Ogg1. Interestingly, the effects of the *XRS2* deletion were almost completely suppressed by the additional deletion of *NTG1* and *NTG2*. In conclusion, our data suggested that the MRX complex acts downstream of Ntg1 and Ntg2 in the AP-lyase-mediated repair pathway and that intermediates resulting from incomplete processing in this pathway due to the *XRS2* deletion were more severe than blocking the whole subpathway. In addition to the current model, our data suggest that in this pathway short-patch and long-patch repair products were synthesized instead of short-patch products only.

The lack of influence of *XRS2* on the incision assay demonstrated that base recognition and the generation of single-strand breaks were independent of *XRS2* and put the role of the MRX complex downstream of damage recognition and strand incision, which fitted with the fact that both, the repair of a uracil-containing and an 8-oxoG-containing oligonucleotide, were affected in the *xrs2* mutant. Most likely, the role of the MRX complex is the enabling of an efficient polymerase activity. This assumption was substantiated by two findings: (i) the gap-filling assay directly showed that protein extracts from the *xrs2* mutant display a decreased polymerization activity and (ii) the inhibition of polymerases by aphidicoline demonstrated that a major part of DNA synthesis in BER was executed by an aphidicoline-sensitive polymerase(s) in wildtype, whereas aphidicoline treatment had no impact in *xrs2* extracts, indicating that this (these) polymerase(s) was already inactive as a consequence of the *XRS2* deletion.

In mammalian cells, the WRN protein, a member of the RecQ helicase family, was demonstrated to activate BER by interacting with key players of this pathway. WRN cooperated especially with Polβ, the most important polymerase for BER in mammalian cells that is needed for the insertion of the first nucleotide in the gap-filling step (44,52). WRN also interacts with Nbs1 (53), the mammalian homolog of Xrs2, which was recently shown

to be involved in BER (54). The authors suggested a role of Nbs1 in the recruitment step of Polβ. In yeast cells it was already shown that the RecQ helicase Sgs1 forms a complex with Mre11 following MMS treatment (55). We speculate that, like in mammalian cells, a large complex, composed of MRX and further BER factors, is needed to activate BER by managing the recruitment of polymerases for the repair process. Our results demonstrate that the MRX complex is a requisite for the efficient repair of DNA base damage, in addition to its better-known functions in DNA DSB repair. Further studies will be needed to identify the exact role and the interaction partners of the MRX complex in the BER pathway.

FUNDING

Funding for open access charge: Helmholtz Centre Munich—German Research Centre for Environmental Health.

Conflict of interest statement. None declared.

REFERENCES

1. Friedberg,E.C. (2003) DNA damage and repair. *Nature*, **421**, 436–440.
2. Lindahl,T. (1993) Instability and decay of the primary structure of DNA. *Nature*, **362**, 709–715.
3. Cadet,J., Berger,M., Douki,T. and Ravanat,J.L. (1997) Oxidative damage to DNA: formation, measurement, and biological significance. *Rev. Physiol. Biochem. Pharmacol.*, **131**, 1–87.
4. Boiteux,S., Gellon,L. and Guibourt,N. (2002) Repair of 8-oxoguanine in Saccharomyces cerevisiae: interplay of DNA repair and replication mechanisms. *Free Radic. Biol. Med.*, **32**, 1244–1253.
5. Beranek,D.T. (1990) Distribution of methyl and ethyl adducts following alkylation with monofunctional alkylating agents. *Mutat. Res.*, **231**, 11–30.
6. Guillet,M. and Boiteux,S. (2003) Origin of endogenous DNA abasic sites in Saccharomyces cerevisiae. *Mol. Cell. Biol.*, **23**, 8386–8394.
7. Wilson,D.M. III and Bohr,V.A. (2007) The mechanics of base excision repair, and its relationship to aging and disease. *DNA Repair (Amst.)*, **6**, 544–559.
8. Krokan,H.E., Standal,R. and Slupphaug,G. (1997) DNA glycosylases in the base excision repair of DNA. *Biochem. J.*, **325 (Pt 1)**, 1–16.
9. Ramotar,D., Popoff,S.C., Gralla,E.B. and Demple,B. (1991) Cellular role of yeast Apn1 apurinic endonuclease/3′-diesterase: repair of oxidative and alkylation DNA damage and control of spontaneous mutation. *Mol. Cell. Biol.*, **11**, 4537–4544.
10. Sander,M. and Ramotar,D. (1997) Partial purification of Pde1 from Saccharomyces cerevisiae: enzymatic redundancy for the repair of 3'-terminal DNA lesions and abasic sites in yeast. *Biochemistry*, **36**, 6100–6106.
11. Wu,X. and Wang,Z. (1999) Relationships between yeast Rad27 and Apn1 in response to apurinic/apyrimidinic (AP) sites in DNA. *Nucleic Acids Res.*, **27**, 956–962.
12. Kao,H.I., Henricksen,L.A., Liu,Y. and Bambara,R.A. (2002) Cleavage specificity of Saccharomyces cerevisiae flap endonuclease 1 suggests a double-flap structure as the cellular substrate. *J. Biol. Chem.*, **277**, 14379–14389.
13. Boiteux,S. and Guillet,M. (2004) Abasic sites in DNA: repair and biological consequences in Saccharomyces cerevisiae. *DNA Repair (Amst.)*, **3**, 1–12.
14. Girard,P.M. and Boiteux,S. (1997) Repair of oxidized DNA bases in the yeast Saccharomyces cerevisiae. *Biochimie*, **79**, 559–566.
15. Alseth,I., Eide,L., Pirovano,M., Rognes,T., Seeberg,E. and Bjoras,M. (1999) The Saccharomyces cerevisiae homologues of endonuclease III from Escherichia coli, Ntg1 and Ntg2, are both required for efficient repair of spontaneous and induced oxidative DNA damage in yeast. *Mol. Cell. Biol.*, **19**, 3779–3787.
16. Alseth,I., Osman,F., Korvald,H., Tsaneva,I., Whitby,M.C., Seeberg,E. and Bjoras,M. (2005) Biochemical characterization and DNA repair pathway interactions of Mag1-mediated base excision repair in Schizosaccharomyces pombe. *Nucleic Acids Res.*, **33**, 1123–1131.
17. Wang,Z., Wu,X. and Friedberg,E.C. (1993) DNA repair synthesis during base excision repair in vitro is catalyzed by DNA polymerase epsilon and is influenced by DNA polymerases alpha and delta in Saccharomyces cerevisiae. *Mol. Cell. Biol.*, **13**, 1051–1058.
18. Blank,A., Kim,B. and Loeb,L.A. (1994) DNA polymerase delta is required for base excision repair of DNA methylation damage in Saccharomyces cerevisiae. *Proc. Natl Acad. Sci. USA*, **91**, 9047–9051.
19. Tsukuda,T., Fleming,A.B., Nickoloff,J.A. and Osley,M.A. (2005) Chromatin remodelling at a DNA double-strand break site in Saccharomyces cerevisiae. *Nature*, **438**, 379–383.
20. Lisby,M., Barlow,J.H., Burgess,R.C. and Rothstein,R. (2004) Choreography of the DNA damage response: spatiotemporal relationships among checkpoint and repair proteins. *Cell*, **118**, 699–713.
21. Ivanov,E.L., Sugawara,N., White,C.I., Fabre,F. and Haber,J.E. (1994) Mutations in XRS2 and RAD50 delay but do not prevent mating-type switching in Saccharomyces cerevisiae. *Mol. Cell. Biol.*, **14**, 3414–3425.
22. Grenon,M., Gilbert,C. and Lowndes,N.F. (2001) Checkpoint activation in response to double-strand breaks requires the Mre11/Rad50/Xrs2 complex. *Nat. Cell Biol.*, **3**, 844–847.
23. Daley,J.M., Palmbos,P.L., Wu,D. and Wilson,T.E. (2005) Nonhomologous end joining in yeast. *Annu. Rev. Genet.*, **39**, 431451.
24. Steininger,S., Gomez-Paramio,I., Braselmann,H., Fellerhoff,B., Dittberner,D., Eckardt-Schupp,F. and Moertl,S. (2008) Xrs2 facilitates crossovers during DNA double-strand gap repair in yeast. *DNA Repair (Amst)*, **7**, 1563–1577.
25. D'Amours,D. and Jackson,S.P. (2002) The Mre11 complex: at the crossroads of DNA repair and checkpoint signalling. *Nat. Rev. Mol. Cell Biol.*, **3**, 317–327.
26. Mallory,J.C., Bashkirov,V.I., Trujillo,K.M., Solinger,J.A., Dominska,M., Sung,P., Heyer,W.D. and Petes,T.D. (2003) Amino acid changes in Xrs2p, Dun1p, and Rfa2p that remove the preferred targets of the ATM family of protein kinases do not affect DNA repair or telomere length in Saccharomyces cerevisiae. *DNA Repair (Amst.)*, **2**, 1041–1064.
27. Chang,M., Bellaoui,M., Boone,C. and Brown,G.W. (2002) A genome-wide screen for methyl methanesulfonate-sensitive mutants reveals genes required for S phase progression in the presence of DNA damage. *Proc. Natl Acad. Sci. USA*, **99**, 16934–16939.
28. Letavayova,L., Markova,E., Hermanska,K., Vlckova,V., Vlasakova,D., Chovanec,M. and Brozmanova,J. (2006) Relative contribution of homologous recombination and non-homologous end-joining to DNA double-strand break repair after oxidative stress in Saccharomyces cerevisiae. *DNA Repair (Amst)*, **5**, 602–610.
29. Tucker,C.L. and Fields,S. (2004) Quantitative genome-wide analysis of yeast deletion strain sensitivities to oxidative and chemical stress. *Comp Funct Genom*, **5**, 216–224.
30. Huang,M.E., Rio,A.G., Nicolas,A. and Kolodner,R.D. (2003) A genomewide screen in Saccharomyces cerevisiae for genes that suppress the accumulation of mutations. *Proc. Natl Acad. Sci. USA*, **100**, 11529–11534.
31. Lundin,C., North,M., Erixon,K., Walters,K., Jenssen,D., Goldman,A.S. and Helleday,T. (2005) Methyl methanesulfonate (MMS) produces heat-labile DNA damage but no detectable in vivo DNA double-strand breaks. *Nucleic Acids Res.*, **33**, 3799–3811.
32. Hendricks,C.A., Razlog,M., Matsuguchi,T., Goyal,A., Brock,A.L. and Engelward,B.P. (2002) The S. cerevisiae Mag1

3-methyladenine DNA glycosylase modulates susceptibility to homologous recombination. *DNA Repair (Amst.)*, **1**, 645–659.
33. Paques,F. and Haber,J.E. (1999) Multiple pathways of recombination induced by double-strand breaks in Saccharomyces cerevisiae. *Microbiol. Mol. Biol. Rev.*, **63**, 349–404.
34. Xiao,W., Chow,B.L. and Rathgeber,L. (1996) The repair of DNA methylation damage in Saccharomyces cerevisiae. *Curr. Genet.*, **30**, 461–468.
35. Knop,M., Siegers,K., Pereira,G., Zachariae,W., Winsor,B., Nasmyth,K. and Schiebel,E. (1999) Epitope tagging of yeast genes using a PCR-based strategy: more tags and improved practical routines. *Yeast*, **15**, 963–972.
36. Wach,A., Brachat,A., Pohlmann,R. and Philippsen,P. (1994) New heterologous modules for classical or PCR-based gene disruptions in Saccharomyces cerevisiae. *Yeast*, **10**, 1793–1808.
37. Myslinski,E., Segault,V. and Branlant,C. (1990) An intron in the genes for U3 small nucleolar RNAs of the yeast Saccharomyces cerevisiae. *Science*, **247**, 1213–1216.
38. Schiestl,R.H. and Gietz,R.D. (1989) High efficiency transformation of intact yeast cells using single stranded nucleic acids as a carrier. *Curr. Genet.*, **16**, 339–346.
39. Melo,R.G., Leitao,A.C. and Padula,M. (2004) Role of OGG1 and NTG2 in the repair of oxidative DNA damage and mutagenesis induced by hydrogen peroxide in Saccharomyces cerevisiae: relationships with transition metals iron and copper. *Yeast*, **21**, 991–1003.
40. Pohlit,W. and Heyder,I.R. (1977) Growth of cells on solid culture medium. II. Cell physiological data of stationary yeast cells and the initiation of cell cycle in nutrient free buffer solution. *Radiat. Environ. Biophys.*, **14**, 213–230.
41. Dardalhon,M., Nohturfft,A., Meniel,V. and Averbeck,D. (1994) Repair of DNA double-strand breaks induced in Saccharomyces cerevisiae using different gamma-ray dose-rates: a pulsed-field gel electrophoresis analysis. *Int. J. Radiat. Biol.*, **65**, 307–314.
42. Frankenberg-Schwager,M., Frankenberg,D., Blocher,D. and Adamczyk,C. (1980) Repair of DNA double-strand breaks in irradiated yeast cells under nongrowth conditions. *Radiat. Res.*, **82**, 498–510.
43. Friedl,A.A., Kraxenberger,A. and Eckardt-Schupp,F. (1995) Use of pulsed-field gel electrophoresis for studies of DNA double-strand break repair in the yeast Saccharomyces cerevisiae. *Methods: A Companion to Methods in Enzymology*, **7**, 205–218.
44. Harrigan,J.A., Wilson,D.M. III, Prasad,R., Opresko,P.L., Beck,G., May,A., Wilson,S.H. and Bohr,V.A. (2006) The Werner syndrome protein operates in base excision repair and cooperates with DNA polymerase beta. *Nucleic Acids Res.*, **34**, 745–754.
45. Wang,Z., Wu,X. and Friedberg,E.C. (1997) Molecular mechanism of base excision repair of uracil-containing DNA in yeast cell-free extracts. *J. Biol. Chem.*, **272**, 24064–24071.
46. Wyatt,M.D. and Pittman,D.L. (2006) Methylating agents and DNA repair responses: methylated bases and sources of strand breaks. *Chem. Res. Toxicol.*, **19**, 1580–1594.
47. Ma,W., Resnick,M.A. and Gordenin,D.A. (2008) Apn1 and Apn2 endonucleases prevent accumulation of repair-associated DNA breaks in budding yeast as revealed by direct chromosomal analysis. *Nucleic Acids Res.*, **36**, 1836–1846.
48. Kelley,M.R., Kow,Y.W. and Wilson,D.M. III (2003) Disparity between DNA base excision repair in yeast and mammals: translational implications. *Cancer Res.*, **63**, 549–554.
49. Krogh,B.O. and Symington,L.S. (2004) Recombination proteins in yeast. *Annu. Rev. Genet.*, **38**, 233–271.
50. Tsukamoto,Y., Mitsuoka,C., Terasawa,M., Ogawa,H. and Ogawa,T. (2005) Xrs2p regulates Mre11p translocation to the nucleus and plays a role in telomere elongation and meiotic recombination. *Mol. Biol. Cell*, **16**, 597–608.
51. Palmbos,P.L., Daley,J.M. and Wilson,T.E. (2005) Mutations of the Yku80 C terminus and Xrs2 FHA domain specifically block yeast nonhomologous end joining. *Mol. Cell. Biol.*, **25**, 10782–10790.
52. Das,A., Boldogh,I., Lee,J.W., Harrigan,J.A., Hegde,M.L., Piotrowski,J., de Souza Pinto,N., Ramos,W., Greenberg,M.M., Hazra,T.K. *et al.* (2007) The human Werner syndrome protein stimulates repair of oxidative DNA base damage by the DNA glycosylase NEIL1. *J. Biol. Chem.*, **282**, 26591–26602.
53. Cheng,W.H., von Kobbe,C., Opresko,P.L., Arthur,L.M., Komatsu,K., Seidman,M.M., Carney,J.P. and Bohr,V.A. (2004) Linkage between Werner syndrome protein and the Mre11 complex via Nbs1. *J. Biol. Chem.*, **279**, 21169–21176.
54. Sagan,D., Muller,R., Kroger,C., Hematulin,A., Mortl,S. and Eckardt-Schupp,F. (2009) The DNA repair protein NBS1 influences the base excision repair pathway. *Carcinogenesis*, **30**, 408–415.
55. Chiolo,I., Carotenuto,W., Maffioletti,G., Petrini,J.H., Foiani,M. and Liberi,G. (2005) Srs2 and Sgs1 DNA helicases associate with Mre11 in different subcomplexes following checkpoint activation and CDK1-mediated Srs2 phosphorylation. *Mol. Cell. Biol.*, **25**, 5738–5751.